Electronic properties of the AlAs-GaAs (001) interface and superlattice

J. N. Schulman and T. C. McGill
California Institute of Technology, Pasadena, California 91125
(Received 29 January 1979)

The tight-binding method is used to calculate the band structure and the character of the electronic states of the AlAs-GaAs (001) superlattice.The nature and value of the energy gap as a function of slab thickness is calculated.In the limit in which the thickness of the repeated superlattice slab becomes large, the system approximates a series of simple interfaces between AlAs and GaAs. This system is studied in detail, with special emphasis placed on the determination of interface states. Layer energy densities of states and charge densities per layer are found for different slab thicknesses. The electronic character of the atomic layers not directly adjacent to the interfaces closely resembles that of the bulk semiconductors in terms of anion and cation charge densities and total squared amplitude in s and p orbitals.

I. INTRODUCTION

In recent years superlattices of alternating GaAs and AlAs layers have been fabricated using molecular beam epitaxy.[1,2] These superlattices are a new physical material for experimental and theoretical study. Since the superlattices consist of interfaces between GaAs and AlAs, they offer an opportunity to investigate the properties of these interfaces as well as the superlattice itself.

This system is suitable for theoretical study of superlattices since the structure may closely approximate a simple ideal model. The two materials have the same crystal structure and they have lattice constants which differ by about 0.1%. Hence, the structures tend to form with a minimum amount of defecting at the interface. The similar chemical nature of the Ga and Al atoms makes it likely that there is not a large amount of relaxation of the atoms at the interface. The small interdiffusion coefficients reported for Ga and Al in this system[3,4] and Raman scattering studies of the phonon spectrum[5] suggest that the interface is rather abrupt. For these reasons we approximate this system by an abrupt interface between the AlAs and GaAs with structures which are ideal.

As the ability to fabricate and analyze molecular-beam-epitaxy-grown materials has improved, attempts have been made to measure their more complex properties. Superlattice effects on electron and phonon energy levels have been extensively investigated. Most experiments were analyzed using a simple theory. AlAs, having an indirect band gap of 2.25 eV at 0 °K, is envisioned as forming a series of barriers to electrons and holes in the GaAs, which has a smaller direct gap (Fig. 1). The conduction- and valence-band discontinuities (ΔE_c and ΔE_v), which form the sides of the barriers, must be determined. Dingle, Wiegmann, and Henry[6] measured the splitting in the optical-absorption spectra of two peaks due to transitions from electrons in the lowest GaAs conduction-band well state to the light and to the heavy hole states in the GaAs valence-band well. They fit this splitting using a valence-band discontinuity equal to 15% of the energy-gap difference between GaAs and $Al_xGa_{1-x}As$. The samples they used had x values less than 0.35, resulting in direct $Al_xGa_{1-x}As$. In determining the discontinuities in our case, in which $x=1$ and $Al_xGa_{1-x}As$ is indirect, we assumed that the 15% gap difference applied to the direct gap differences. Efforts to predict the band discontinuities *a priori* using more detailed pseudopotential methods have so far not been successful for AlAs-GaAs.[7]

The electrons and holes in the well models were assumed to have effective masses which were related to their bulk GaAs values. Mukherji and Nag[8] used a somewhat more complicated model which took into account the nonparabolicity of the bands and also the relevant band structure of the $Al_xGa_{1-x}As$ layers which made up the sides of the wells. Recently two pseudopotential calculations have been done with somewhat conflicting results concerning the location and nature of the lowest conduction band in the alternating monolayer superlattice.[9,10] Section IV discusses these results.

The abruptness of the sides of the wells is made uncertain by two factors. First, as previously stated, samples having completely abrupt transitions between AlAs and GaAs cannot be made. It may take several angstroms to complete the transition. This is especially crucial for superlattices having small repeat distances where the interface layers are a substantial proportion of the total crystal. Second, the charge transfer between AlAs and GaAs layers may take place over several atomic layers. The resulting dipole layer would form an inclined side to the well. Our calculations shown below indicate that the charge transfer, cal-

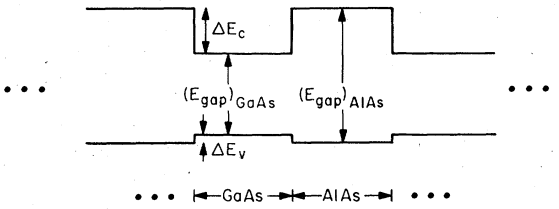

FIG. 1. Well model of AlAs/GaAs superlattice. The smaller band-gapped GaAs forms wells between AlAs barriers for the electrons and holes near the band edges. ΔE_v and ΔE_c are the valence- and conduction-band discontinuities between the AlAs and GaAs.

culated non-self-consistently, is small and occurs between atomic layers adjacent to each interface only. The other layers show bulk characteristics rather quickly away from the interface. The layer densities of states and charge densities of these layers resemble those for bulk GaAs and AlAs. This justifies modeling the system as consisting of a series of wells derived from bulk band discontinuities, especially for superlattices consisting of more than one or two atomic monolayers per slab.

We have done tight-binding calculations for superlattices with alternating slabs of various thicknesses. In the succeeding sections we will report the details of these calculations and the most important properties observed from them. Sections II and III review the tight-binding method and how it applies to the semiconductor-semiconductor interface and superlattice. The procedure used to obtain matrix element parameters is also described. Section IV describes results pertaining to the band-gap behavior and character of the valence- and conduction-band states near the band-gap edges as a function of slab thickness. The results for the case of alternating atomic monolayers of AlAs and GaAs will be compared to the random-alloy band structure. The existence and location of interface states are discussed in Sec. V. Finally, Sec. VI deals with the question of charge transfer and the close to bulklike nature of layers near the interface as determined by the layer density of states.

II. TIGHT-BINDING BULK BAND-STRUCTURE CALCULATION

The basic method we have used is similar to that used in previous surface band-structure calculations for diamond and zinc-blende structures. The important difference is that now there are two types of semiconductors forming the interface replacing the semiconductor-vacuum interface. The two-dimensional periodicity parallel to the interface is preserved. The interface is repeated, therefore avoiding the problem of additional semiconductor-vacuum interfaces. This forms the semiconductor-semiconductor superlattice.

The tight-binding matrix elements of the superlattice matrix are taken over directly from bulk values. These values are determined separately for AlAs and GaAs by adjusting them to reproduce certain low-temperature bulk energy levels. The valence-band discontinuity equal to 15% of the direct-gap differences is then subtracted from the four AlAs diagonal bulk parameters. The resulting parameters are listed in Ref. 11. The bulk energy values used were gotten from two pseudopotential calculations: one by Hess *et al.* for AlAs,[12] and a nonlocal calculation by Chelikowsky and Cohen for GaAs.[13] The pseudopotential and resulting tight-binding energies are listed in Table I.

A total of eight tight-binding wave functions per unit cell were used in the bulk calculation, giving an 8×8 matrix to be diagonalized for the energy eigenvalues and eigenvectors. One s-type wave function and three p-type wave functions (P_x, P_y, P_z) were used for both the anion (As) and for the cation (Al, Ga). The eight wave functions produced four valence bands and four conduction bands, each band being doubly degenerate as the spin-orbit interaction was neglected. All possible nearest-neighbor matrix element parameters were included. Symmetry considerations reduced the number of such parameters in zinc-blende ma-

TABLE I. Tight-binding and pseudopotential eigenvalues used in the parameter fitting procedure. Energies are in eV.

	AlAs		GaAs	
Level	Tight-binding	Ref. 12	Tight-binding	Ref. 13
Γ_1^v	−12.06	−11.66	−12.89	−12.55
Γ_{15}^v	0	0	0	0
Γ_1^c	2.82	3.21	1.53	1.51
Γ_{15}^c	4.19	4.57	3.91	4.55
X_1^v	−9.46	−9.42	−9.96	−9.83
X_3^v	−5.02	−5.55	−6.08	−6.88
X_5^v	−1.72	−1.97	−2.94	−2.99
X_1^c	2.30	2.25	2.07	2.03
X_3^c	3.01	2.62	2.88	2.38
L_1^v	−9.94	−10.07	−10.42	−10.60
L_2^v	−5.85	−5.52	−7.19	−6.83
L_3^v	−0.48	−0.70	−1.28	−1.42
L_1^c	2.64	2.76	1.89	1.82
L_3^c	4.81	5.15	5.78	5.47

terials to nine. The valence bands were fit well with just these parameters. To improve the conduction-band fit, particularly the shapes of the bands, additional second-nearest-neighbor parameters were included. The use of d orbitals would be necessary to improve the conduction bands further.[14] These parameters are an improvement over the parameters previously used by the authors,[15] especially as they affect the lowest conduction band. The resulting bulk band structures are shown in Ref. 11. Comparison of our bulk results with those of Refs. 12 and 13 show good agreement, even with the lower conduction bands. The tight-binding calculation is unable to produce as much curvature in the conduction bands as the pseudopotential calculations although the general shapes are accurate.

III. SUPERLATTICE CALCULATION

Once the bulk tight-binding parameters are determined, the tight-binding matrix for the superlattice using them can be formed. Its form is very similar to that used in previous surface calculations as, for example, by Hirabayashi.[16] The matrix is organized in eight × eight blocks (Fig. 2) representing the integrals between tight-binding orbitals centered on the same and different atomic layers. Each layer contains a single anion and cation per unit cell with four orbitals each. Because only integrals up to second nearest neighbors are used, there are just two types of eight by eight blocks. The blocks down the diagonal (labeled A and a) contain matrix elements between orbitals within a layer including the eight self-energy integrals between a given orbital and itself. The four AlAs self-energy parameters have the previously discussed valence-band discontinuity value subtracted off from them. Matrix elements between adjacent layers (labeled B, b, and β) are located in blocks that are just off-diagonal and in one extra block each at the upper right hand corner and lower left-hand corner. The corner blocks contain the integrals between adjacent layers where each layer is in an adjacent slab. These blocks are the major difference between this matrix and the matrix used for surface calculations. With its matrix elements equal to zero, the surface tight-binding matrix results. It also incorporates an extra phase factor of $e^{ik_z d}$, where d is the slab width and k_z is the component of the k vector perpendicular to the interface. Letting M equal the number of AlAs layers per slab and N the number of GaAs layers per slab, the total size of the superlattice matrix is $[(M+N)\times 8]^2$.

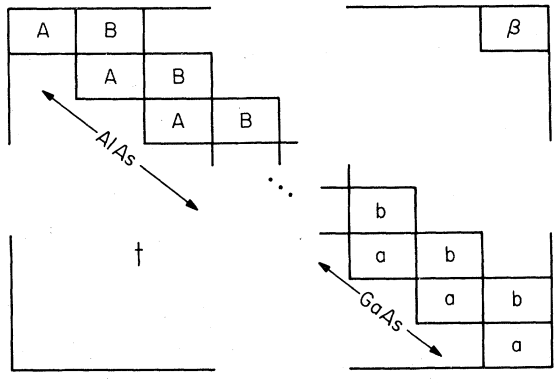

FIG. 2. Superlattice tight-binding matrix. Each block represents an eight × eight submatrix. The upper right-hand corner block, "β", links AlAs and GaAs slabs and has both types of parameters. The matrix is organized such that each block has matrix elements between orbitals centered on atoms in the same (A and a) or adjacent (B, b, or β) superlattice layers.

The AlAs and GaAs share common As ions right at the interface. There is therefore no problem determining the matrix elements at the nearest-neighbor level there. The bulk values were used. Second-nearest-neighbor matrix elements, however, connect Al- and Ga-centered orbitals. The bulk fitting procedure does not supply parameters in this case. Instead, a simple average of Al to Al and Ga to Ga parameters was used. Also, the As to As second-nearest-neighbor parameters were somewhat different in the AlAs and the GaAs. Again an average was used. The lattice match of the interface was assumed to be perfect. No relaxation or reconstruction was assumed.

The eigenvalues and eigenvectors obtained from diagonalizing the tight-binding matrix can be used to calculate an approximate layer density of states for the superlattice. An exact layer density of states cannot be found due to the fact that the wave functions are unknown. Only the coefficients of the localized orbitals that make up the wave functions are available. Although these orbitals might have nonzero amplitudes on layers other than those on which they are centered, it is assumed that this spreading is small and is thus neglected. The layer density of states in a given energy interval and layer is calculated by summing the squares of the localized orbital coefficients centered on that layer for wave functions whose energies are within the energy interval. We used several thousand energies calculated at points in k space throughout the Brillouin zone and binned with an energy resolution of 0.1 eV. An approximate layer valence-charge density can also be calculated by summing up the layer density of states for all the valence-band energies.

IV. PROPERTIES NEAR BAND EDGES

Both bulk AlAs and bulk GaAs are semiconductors, having band gaps of 2.25 eV[12] (indirect) and 1.51 eV[13] (direct), respectively. When AlAs and GaAs are deposited alternately in a superlattice, the resulting structure has some properties which are intermediate between the bulk materials and some completely new properties. In particular, the superlattice material is still found to be semiconducting, but it does not resemble the $Al_xGa_{1-x}As$ alloy of the same Al concentration. This is true even for very thin alternating slabs. Figure 3 shows the behavior of the superlattice band gaps as a function of the number of atomic monolayers of GaAs (N) per repeated slab. The energy gaps at three points in k space are plotted: Γ, J, and K (see inset). The curve labeled Γ represents the direct gap. In the coordinate system whose axes are parallel to the edges of the conventional zinc-blende unit cell of side length a, J has the coordinates $(2\pi/a)$ (0.5, 0.5, 0). The z axis is taken to be perpendicular to the superlattice slabs. The J point has what would correspond to the bulk zinc-blende L point $[2\pi/a(0.5, 0.5, 0.5)]$ folded into it when $\frac{1}{2}(M+N)$ is even. For both AlAs and GaAs, there is a local minimum in the bottom-most conduction band near the L point. The J point is also a local minimum in the superlattice case. The same is true of the K point which has the zinc-blende X point $[(2\pi/a)(1, 0, 0)]$ mapped onto it. The lowest of the curves in Fig. 3 for a given slab thickness determines whether the material is direct or indirect. The band gaps are all relative to the valence-band maxima of the superlattices. Three cases are shown in Fig. 3 for three different ratios of AlAs to GaAs slab thicknesses: (a) 1:2, (b) 1:1, (c) 2:1. This corresponds to values of x for the $Al_xGa_{1-x}As$ alloy of $\frac{1}{3}$, $\frac{1}{2}$, and $\frac{2}{3}$. As the number of GaAs monolayers per slab increases, the gap values approach their bulk GaAs values of 1.5 eV for Γ, 2.1 eV for X, and 1.9 eV for L. The values calculated for the thickest GaAs slab are shown in Fig. 3(a) for $N=12$. The Γ and J gaps (1.7 and 2.0 eV) are still not very close to their bulk values. The K-point gap, however, is seen to be uniformly flat for all N. This is because the bulk X-point conduction-band energies of AlAs and GaAs relative to their valence-band maxima are separated by an amount approximately equal to the valence-band off-set (0.19 eV) between the two materials. When this off-set is subtracted from the AlAs diagonal parameters, as previously described, the energies at the two bulk X-points are approximately the same. There is, therefore, no well confining the electrons to either the AlAs or GaAs slabs. This is confirmed by examining the state at this energy. In Fig. 4 is plotted the total squared amplitude on the anion and cation at each layer for the case $M=5$, $N=10$. Layers labeled 1–5 are AlAs and layers 6–15 are GaAs. It is highly uniform in the direction perpendicular to the interface with close to the same amplitudes on AlAs and GaAs. Both the Γ- and L-point conduction-band energies, by contrast, are higher in AlAs. This tends to confine the electrons to the GaAs slabs. Thicker slabs mean wider wells and therefore lower ground-state well energies.

A typical set of GaAs band-gap edge well-like states at the Γ point is shown in Fig. 5. In this case ten layers of AlAs alternate with ten layers of GaAs. Five different energies are shown in Figs. 5(a)–5(e), in order of increasing energy. The states shown in Figs. 5(b) and 5(c) with energies −0.074 and −0.052 eV form a triplet of states (including the double degeneracy of the −0.052-eV state) originating from the triply degenerate zinc-blende Γ_{15} symmetry state. The disruption of

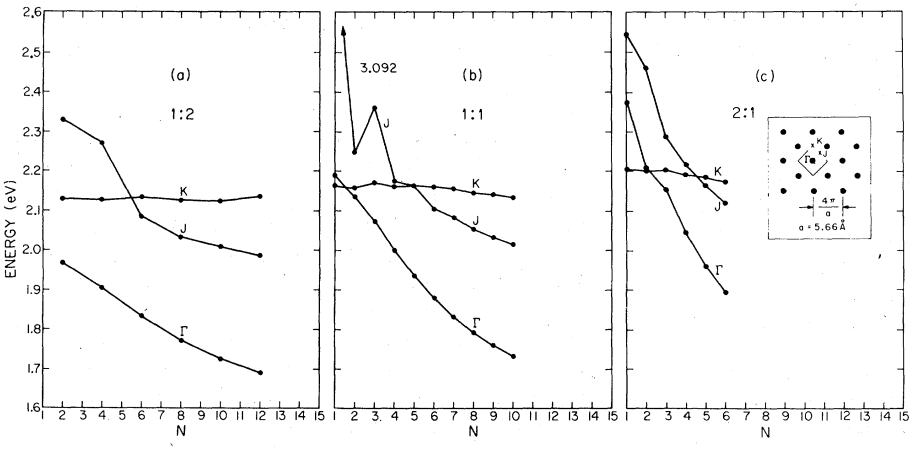

FIG. 3. Energy gaps from the top of the valence band to the lowest conduction-band energies at Γ, J, and K. The location of these points in the slice of k space parallel to the interfaces is shown in the inset of (c). N is the number of atomic monolayers of GaAs per repeated slab. Three ratios of AlAs to GaAs slab thicknesses (M:N) are shown: (a) 1:2, (b) 1:1, (c) 2:1.

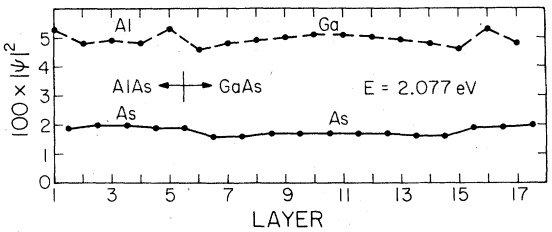

FIG. 4. Anion (As) and cation (Al and Ga) charge distributions for the state at the conduction-band minimum at K for the superlattice consisting of five layers of AlAs alternating with ten layers of GaAs. Separate curves for the anion and cation are given. The numbers on the horizontal axis label the cation (Al, Ga) positions.

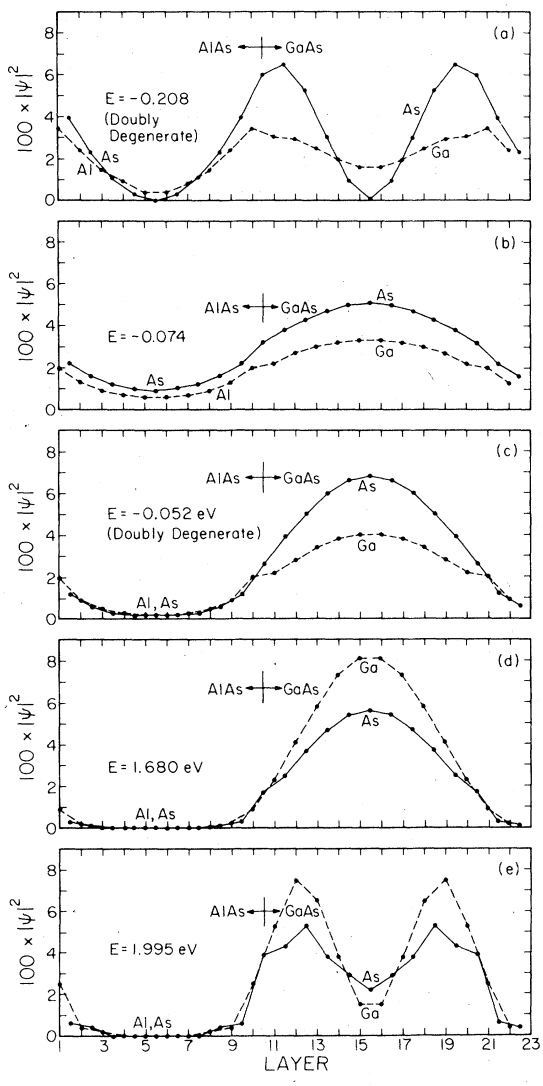

FIG. 5. Charge distributions for five states with energies as shown at Γ for the superlattice consisting of ten layers of AlAs alternating with ten layers of GaAs.

periodicity in the z direction splits off one state leaving the states with x- and y-type symmetry degenerate. These three states all have the characteristic single-peaked shape of the lowest-well-potential eigenfunction. Figure 5(a) shows the double-peaked structure characteristic of the next-well-potential eigenfunction. The next state lower in energy (not shown) is located mostly on the AlAs layers. The situation is similar for the conduction-band states in Figs. 5(d) and 5(e). Both single- and double-peaked eigenfunctions are found. There are other well-like states with energies above these.

The electronic states formed when *very* thin slabs of AlAs and GaAs are alternated in a superlattice are more difficult to analyze. The energy gap at the K point remains nearly constant in all three cases shown in Fig. 3 as previously explained. The J-point curve in Fig. 3(b) is no longer monotonic for small N. This is explained by examining in detail which bulk states are mapped onto the J point. These are states with bulk k values of $(2\pi/a)(\frac{1}{2},\frac{1}{2},2n/I)$, where I is the total number of layers of AlAs plus GaAs per slab $(M+N)$ and n takes on the values $1 \rightarrow I$. Therefore it is only for even values of $\frac{1}{2}I$ that the J point includes the bulk L point. It is exactly for these values of N that the J-point curve is lower. The gap values at $N=1$ and 3 are higher because they represent the energies of points in bulk k space near but not at L. The energies at these bulk points are indeed higher than at the L point. As N increases beyond three the J point includes bulk values of k so close to L that their energies are indistinguishable from those at the L point. Results obtained using our previous set of parameters[15] do not show this feature because of the flatness of the bulk conduction bands produced by them. The K point contains bulk k values of $(2\pi/a)(1,0,2n/I)$ and thus includes the X point whenever $n=0$ for any I.

Another interesting feature of Fig. 3 is the direct-indirect transition determined by the relative energy-gap values at Γ and K. The alloy $Al_xGa_{1-x}As$ has an indirect band gap at the X point for values of x greater than about 0.35.[17] The X point is mapped onto the Γ point for even values of I, as the bulk values associated with Γ are given by $(2\pi/a)(0,0,2n/I)$. Thus there are X points mapped onto both Γ and K. In Figs. 3(b) and 3(c) the K-point curve is seen to cross the Γ-point curve for small N, indicating that the X point associated with the K point has a smaller energy there. Examining the state at Γ for the case $N=1$ in Fig. 3(b) reveals that it is of Γ_4 symmetry, which would be the case for an X_1 symmetry bulk state mapped onto the Γ point. The state symmetries for N greater than one are Γ_1-type, con-

TABLE II. Energy values at the bottom of the conduction band calculated using tight-binding parameters. Results are shown at the zinc-blende Γ, X, and L points. The energy of the valence-band maximum is zero in all cases. The point in k space appropriate to the superlattice is shown in parentheses. Energies are in eV. $a = 5.66$ Å.

	Γ	X	L
AlAs	2.83	2.30	2.64
GaAs	1.53	2.07	1.89
Alloy ($x=0.5$)	2.18	2.18	2.27
$M=N=1$ Superlattice	2.19	2.16	2.17
	$(2\pi/a)(0,0,0)$	$(2\pi/a)(1,0,0)$	$(2\pi/a)(\frac{1}{2},\frac{1}{2},\frac{1}{2})$

firming that they originate from bulk Γ_1 symmetry states. Caruthers and Lin-Chung[9] in their pseudopotential calculation find that the Γ_4 state has the lowest conduction-band energy for $M=N=1$ by several tenths of eV's. This is a large departure from what would be expected from considering the bulk band structures or the $Al_{0.5}Ga_{0.5}As$ alloy. Our results are closer to the alloy energies, as calculated by simply averaging the AlAs and GaAs tight-binding parameters. The results of this calculation are shown in Table II. A recent pseudopotential calculation done by Andreoni, Baldereschi, and Car[10] also finds small departures from the alloy case.

V. BAND STRUCTURE AND INTERFACE STATES

The band structure in representative directions of the superlattice consisting of four layers of AlAs alternating with four layers of GaAs is shown in Fig. 6. The two directions perpendicular to the interface have less dispersion than the directions parallel to the interface. This is especially true near the valence-band maxima and the conduction-band minima. In both of the two perpendicular directions there is a slight rise in energy at the bottom of the conduction band toward the Brillouin-zone edge. This feature is held in common with superlattices of other layer thicknesses. In this case the bottom-most conduction-band energy increases by 50 meV from $(2\pi/a)(0,0,0)$ to $(2\pi/a)(0,0,\frac{1}{8})$ and by 190 meV from $(2\pi/a)(1,0,0)$ to $(2\pi/a)(1,0,\frac{1}{8})$.

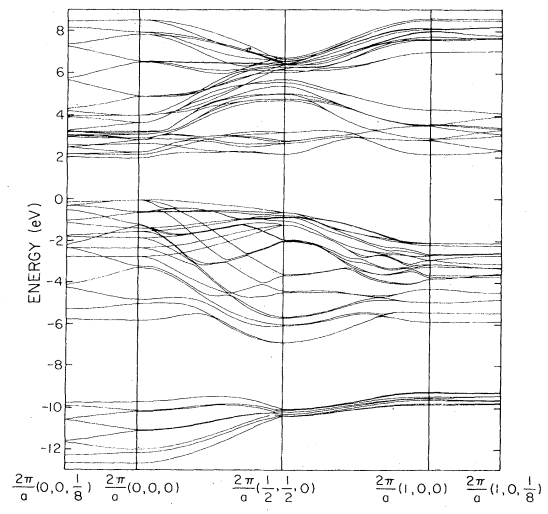

FIG. 6. Band structure of the AlAs-GaAs superlattice consisting of four monolayers of AlAs alternating with four monolayers of GaAs. The quantity a is the length of the side of the conventional zinc-blende unit cell. It equals 5.66 Å.

The superlattice band structure shown in Fig. 6 for a thin slabbed superlattice has no obvious split off bands which might need to be identified with localized states. It can approximately be described as a combination of the AlAs and GaAs three-dimensional bulk bands mapped onto the smaller superlattice reciprocal space. Instead of the eight energy bands (ignoring degeneracy) found in the bulk band structures, there are now $8\times(M+N)$ bands, reflecting the fact that there are $M+N$ as many basis wave functions in the enlarged superlattice unit cell.

For larger slab thicknesses, split off bands characteristic of interface states start to appear. An interface state is here defined as a state having nonzero amplitudes on layers only within two or three layers of the interface. In Fig. 7 are shown the valence bands near the J point for the superlattice with $M=N=10$. Only a small volume in reciprocal-lattice space near the J point is found to have definite interface states. The interface states at the J point are states which are split off from high concentrations of bands. This is shown in Fig. 7, where the heads of arrows indicate the interface states and the tails of arrows indicate the grouping of bands from which these states are split off. All four interface states are located in energy gaps at the J point. No interface states are found within the semiconducting band gap of the superlattice, however. The K point has two or three states which have large squared amplitudes

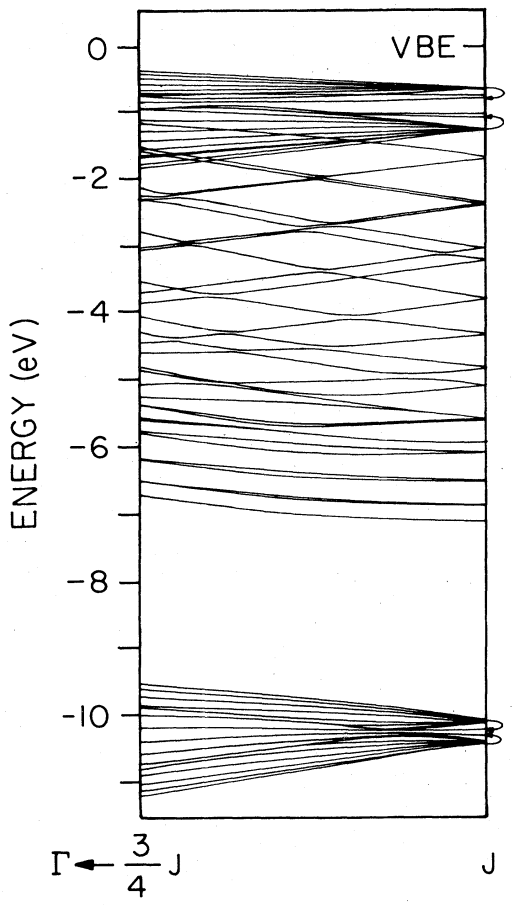

FIG. 7. Valence-band energies near the J-point (from the Γ point) for the $M=N=10$ superlattice. Arrows indicate the interface states and the bands from which they are split off. VBE indicates the valence-band edge.

on the interface layers but which do not go to zero away from the interface. The Γ point has no interface states.

The eigenvectors of the J point whose energies are shown in Fig. 7 show that, except for the interface states indicated, the thick slabbed superlattice can also be described as a superposition of AlAs and GaAs bulk band structures, as would be expected. Most states show pronounced AlAs or GaAs character. The energies of these states are very close to bulk values. The bulk energies corresponding to the J point are found from the bulk 8×8 tight-binding matrix by diagonalizing that matrix for $M+N$ values of the k vector as previously described. By combining the results of this procedure for both AlAs and GaAs, a comparison with the superlattice energies can be made. When the appropriate AlAs and GaAs bulk states are close in energy, a superlattice state occurs which has substantial amplitudes on both the AlAs and GaAs slabs, similar to the previously described K-point conduction-band minimum state.

The four high concentrations of nine bands each from which the four interface states are split off are formed due to the small dispersion of the bulk bands in the z direction away from the bulk L point in both AlAs and GaAs. The dense subbands are formed when the bulk states with different k_z values are superimposed. The eigenvectors of these states reveal them to be almost identical in character to bulk states at the same energies. The interface states are the tenth member of these subbands. The two lowest subbands are related to the AlAs and GaAs bulk L_1^v states at −10.1 and −10.4 eV. The two interface states are split off by about 0.1 eV below the AlAs energy and 0.1 eV above the GaAs energy. The two subbands near the top of the valence band are almost identical in energy to the bulk L_3^v states at −0.67 eV (AlAs) and −1.28 eV (GaAs). The GaAs interface state is split off by 0.2 eV and the AlAs interface state by about 0.15 eV.

VI. DENSITIES OF STATES

The transition of the electronic structure from interface to bulk was investigated using a density-of-states calculation. Figure 8 shows the layer density of states for the $M=N=7$ superlattice for the layers adjacent to the interface and for the layers located in the center of the AlAs and GaAs slabs. Also shown are the densities of states of bulk AlAs and bulk GaAs. The centers of the slabs, layers 4 and 11, are seen to be similar to bulk AlAs and GaAs, respectively. Even the layers right adjacent to the interface, layers 7 and 14, can be identified as being AlAs- or GaAs-like, although they are not as bulk-like. Layers one more removed from the interface (not shown) substantially resemble the bulk. The interface state density is too small to make any noticeable contribution to the density of states in the form of separate peaks.

The charge density can be found by summing up the density of states over the valence band and is shown in Table III. When this is done a charge density per layer much like the bulk results. If bulk AlAs or GaAs were to be divided up into layers like a superlattice, each layer would have exactly four of its eight tight-binding linear combinations filled with electrons (two per band) the same way on each layer. Because of the lack of translational symmetry perpendicular to the interface, there no longer must be the same charge on each layer. Table III gives the corresponding numbers for the $M=N=4$ superlattice broken down to give the components on the anion and cation, and on the s and p orbitals. These numbers differ from the

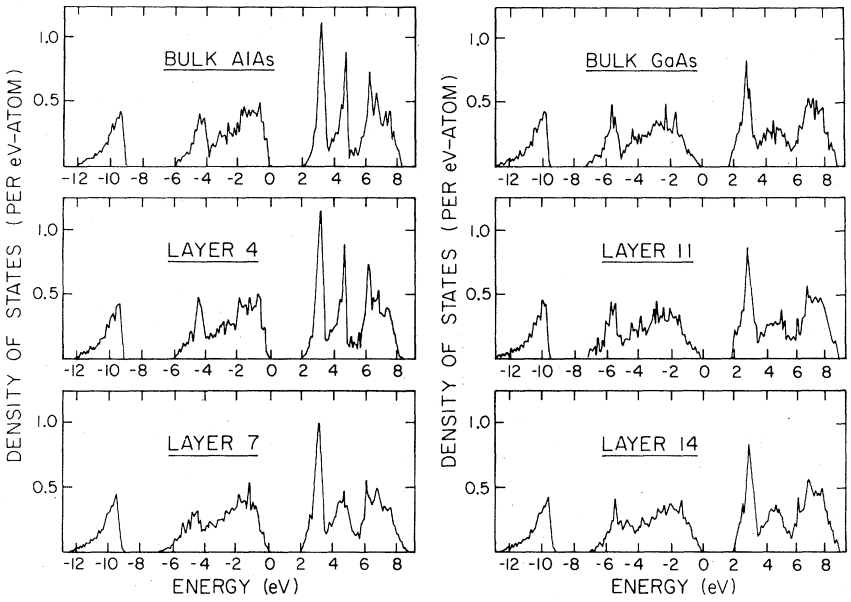

FIG. 8. Densities of states of bulk AlAs, bulk GaAs, and layer densities of states for the $M=N=7$ superlattice. Densities of states are shown for layers adjacent to the interface and at the center of the AlAs and GaAs slabs. The bulk curves integrate to four, the number of states per atom (not including spin).

bulk values only adjacent to the interfaces. The anion to cation ratio and the ratio of s-symmetry to p-symmetry squared amplitudes were also very close to bulk values. Most of the charge shift at the interface is due to a transfer of electrons from the Al to the Ga layers right next to the interface. The As interface layer has just the average charge of the two bulk As layers. Approximating this charge shift as being between two uniformly charged sheets parallel to the interface and located at the Al and Ga atoms results in an energy shift of just 0.21 eV.

VII. CONCLUSIONS

A tight-binding calculation of the AlAs/GaAs superlattice was done in order to study the energy bands and states in more detail than was possible with previous simple models. The variation of the band gap with slab thickness was determined. Interface states were found although none in energy ranges accessible to experimental methods. The superlattice was found to be similar to bulk AlAs and GaAs in several respects except at layers adjacent to the interfaces.

TABLE III. Valence-charge densities for bulk AlAs, bulk GaAs, and the $M=N=4$ superlattice. The rows labeled s, p, and $s+p$ contain the charge densities from the s-like states, the p-like states and the sums of these two, respectively. The bulk charge densities each add up to eight, the number of valence electrons per unit cell. The sums of adjacent $s+p$ values for the superlattice are also close to eight, except near the interface.

	Bulk AlAs			Bulk GaAs	
	Al	As		Ga	As
s	1.08	1.47	s	1.12	1.53
p	2.77	2.68	p	2.43	2.92
$s+p$	3.85	4.15	$s+p$	3.55	4.45

$M=N=4$ superlattice

...	As	Al	As	Al	As	Ga	As	Ga	As ...
s	1.47	1.08	1.47	1.06	1.50	1.14	1.53	1.12	1.53
p	2.68	2.77	2.67	2.71	2.80	2.49	2.92	2.44	2.92
$s+p$	4.15	3.85	4.14	3.77	4.30	3.63	4.45	3.56	4.45
					↑ Interface layer				

ACKNOWLEDGMENTS

We would like to acknowledge the support of the Office of Naval Research and the Army Research Office. One of us (J.N.S.) would like to acknowledge the support provided by an IBM Fellowship. We have profited from a number of discussions with D. L. Smith and G. C. Osbourn. We are grateful to P. Taborek for help in computing.

[1]L. Esaki and L. L. Chang, Crit. Rev. Solid State Sci. 6, 195 (1976).
[2]R. Dingle, Crit. Rev. Solid State Sci. 5, 585 (1975).
[3]L. L. Chang and A. Koma, Appl. Phys. Lett. 29, 138 (1976).
[4]R. Dingle, in *Proceedings of the Thirteenth International Conference on the Physics of Semiconductors, Rome, 1976*, edited by F. G. Fumi (Tipografia Marves, Rome, 1977), p. 65.
[5]J. L. Merz, A. S. Barker, Jr., and A. C. Gossard, Appl. Phys. Lett. 31, 117 (1977).
[6]R. Dingle, W. Wiegmann, and C. H. Henry, Phys. Rev. Lett. 33, 827 (1974).
[7]W. R. Frensley and H. Kroemer, Phys. Rev. B 16, 2642 (1977).
[8]D. Mukherji and B. R. Nag, Phys. Rev. B 12, 4338 (1975).
[9]E. Caruthers and P. J. Lin-Chung, J. Vac. Sci. Technol. 15, 1459 (1978).
[10]W. Andreoni, A. Baldereschi, and R. Car, Solid State Commun. 17, 821 (1978).
[11]G. C. Osbourn and D. L. Smith, Phys. Rev. B (to be published).
[12]E. Hess, I. Topol, K. R. Schulze, H. Neumann, and K. Unger, Phys. Status Solidi B 55, 187 (1973).
[13]J. R. Chelikowsky and M. L. Cohen, Phys. Rev. B 14, 556 (1976).
[14]D. J. Chadi, Phys. Rev. B 16, 3572 (1977).
[15]J. N. Schulman and T. C. McGill, Phys. Rev. Lett. 39, 1680 (1977).
[16]K. Hirabayashi, J. Phys. Soc. Jpn. 27, 1475 (1969).
[17]B. Monemar, K. K. Shih, and G. D. Pettit, J. Appl. Phys. 47, 2604 (1976).